Ionizing Radiation Effect on the Electrical Properties of Metal/ultra-thin Oxide/Semiconductor Structures

Y. Khlifi[(1)], K. Kassmi[(1)]*, A. Aziz[(1)] , F. Olivié[(2)] , G. Sarrabayrouse[(2)] , A. Martinez[(2)]

[(1)] Université Mohamed Premier, Faculté des Sciences, Dépt de Physique, (L.E.A.A), Route Sidi Maafa BP 524, Oujda, Morocco.

[(2)] Laboratoire d'Analyse et d'Architecture des Systèmes (LAAS-CNRS), 7 Avenue du Colonel Roche, Toulouse 31077, France.

This paper deals with the effects of X-ray radiation (7 Mrad (Si) dose) on the electrical properties of Metal/Oxide/Semiconductor (MOS) structures with ultra thin oxide layer (45 Å to 80 Å), P-type semiconductor (Si), and a chromium gate.

These effects are investigated on the Fowler-Nordheim (FN) conduction and the excess current when the MOS structure is biased with a positive gate voltage ($V_g>0$) (inversion regime); and on the breakdown field when electrons are injected from the metal (accumulation regime, $V_g<0$).

By using the theoretical conduction model developed in a previous paper [1], we have found that the FN conduction parameters improve after radiation. We have interpreted this result, by modelling the excess current before and after radiation, by improving the conduction parameters of defects localized in the oxide layer. Thus the defect barrier was increased by 6.5% while the effective area decreased by 68%.

The analysis of the radiation effect on breakdown distribution shows the degradation of the breakdown field after radiation. These results suggest that the ionising radiation can be involved in the formation of another type of defects in the oxide layer that can lead to the breakdown phenomenon but cannot impact the FN conduction mechanism.

I-INTRODUCTION

The reduction of the MOS structure dimension requires an oxide thickness less than 100 Å. These structures are used in sub micron technology as MOS and MOSFET transistors, RAM and EEPROM memories [2,3]. In such devices, the influence of ionising radiation on the electrical properties is a matter of concern particularly with respect to reliability. Indeed, in different situations as in space or in a nuclear environment, the oxide layer of MOS structures may be exposed to high doses of ionising radiation, which is known to introduce traps in the oxide layers [4]. The generation of these traps subsequently results in the degradation of the device electrical properties. However, during device processing, the scaling down of MOS transistors requires the use of X-ray lithography. Thus it is important to understand the effect of radiation on the electrical properties of MOS structures using an ultra thin oxide layer.

Indeed, the influence of radiation on the MOS structures has been extensively investigated. The main results published in the literature show that in the case of thick oxide layers (in excess of 100 Å) the radiation creates positive charges in the oxide layer close to the oxide/semiconductor interface [5], interface states [6-9] and traps of electrons [8]. Also, the degradation of the channel carrier mobility in the MOSFETs has been reported [9], and in [10,11] it has been shown equally that radiation eliminates the defects created at the oxide/semiconductor interface by He^+ [10] or Ar [11] ion implantation in MOS structures.

For thin oxide layers with a thickness lower than 100 Å, the main results show that the radiation effect:

- is negligible with respect to the creation of interface states and charges in the oxide layers [5,12,13],
- induces a leakage current (radiation induced leakage current : RILC) whose mechanism resembles that of the stress induced leakage current (SILC) [4,14,15],
- degrades the breakdown fields [4] essentially for larger structures by the formation of a percolation path between the cathode and the anode in the MOS structure.

In a previous paper [5], we have showed qualitatively by using the classical model of FN conduction [16] that radiation improves conduction parameters in the inversion regime ($V_g > 0$). In the case of electron injection from the metal ($V_g < 0$) and for an oxide layer with a thickness between 40 Å and 110 Å, it has been shown that radiation hardly affects the current-voltage characteristics particularly at high fields. This shows that the radiation fails to create any charge in the oxide layer close to the metal/oxide interface [5].

In this paper, we review the ionising radiation influence on the FN conduction and the excess current, due to defects localized in the oxide layer [17,18], for an inversion regime (electrons injection from the semiconductor). This study is based on the FN current model that takes account of temperature, semiconductor interface degeneracy (the Fermi energy (E_{fs}) being localized in the semiconductor conduction band) and the Schottky effects (TDSEs) [1]. Also, the influence of radiation on the breakdown field obtained from the current-voltage characteristics in the accumulation regime ($V_g<0$) is considered. This study

enables us to analyse the radiation effect on the defect characteristics such as the effective barrier and the effective area, and to determine the relation between the breakdown mechanism and the presence of defects in the oxide layer.
It should be pointed out that in [17-20] the electrical behaviour of the MOS structures before radiation and after ageing by injecting a constant current has been extensively investigated.

II- EXPERIMENTAL PROCEDURES

Samples are capacitors on P-type silicon wafers, <100> oriented, with a doping level (1–3) 10^{15} cm^{-3}. The substrates are prepared using a standard procedure including the growth of a sacrificial oxide layer of 3500 Å thickness followed by etching and cleaning in a bath (HF/ethanol). Growth of the oxide layer of thickness D_i is obtained in a chlorinated atmosphere diluted in nitrogen at 900 °C, followed by annealing at 1050 °C in nitrogen during 30 mn. A chromium gate is then deposited by evaporation, etched and annealed at 450 °C in forming gas.

Tests are carried out on several devices (about a hundred) using capacitance-voltage $C(V_g)$ at high (1MHz) and low (1kHz) frequencies and current–voltage $I(V_g)$ measurements. The capacitance-voltage measurements were taken using an impedance analyser HP4192A (Hewlett-packard). The current–voltage measurements were carried out using an HP4145A semiconductor parameter analyser in the medium sampling mode. $C(V_g)$ measurements enable us to obtain silicon doping and the oxide layer thickness (D_i) [21].

To investigate the behaviour of the MOS structures under radiation, we radiated the structures, without biasing the components, using an X-ray source. This source consists of an electron gun whose beam is focused on a tungsten anti-cathode, and a high-energy generator of 300 kV maximum, of the CGR 300-150 kV, 10-20 mA AEQUIVOLT type, the dose rate delivered being 220 rad min^{-1} under the conditions of use [5] and radiation ranging from 0 to 7 Mrad (Si).

III- RESULTS AND DISCUSSION

III-1- Theoretical model of the FN conduction

In the MOS structure under study, the oxide thickness is lower than 100 Å. In [5], as mentioned in the introduction, the charge stored in the oxide layer is negligible after radiation. So, for modelling the FN current, we use the theoretical model [1], which does not take account of the charges stored in the oxide layer.

To analyse the effect of radiation on the conduction of MOS structures, we reported their conduction properties in [5] before and after radiation according to the classical model [16]:

$$I_{FN}^{o}(E_i,\Phi_{bs}) = S\,K_1^{o}\,E_i^{2}\exp\left(-\frac{K_2^{o}}{E_i}\right) \quad (1)$$

where, E_i : electrical field in the oxide [18], S : structure area.

K_1^{o}, K_2^{o} : pre-exponential and exponential factor that are a function of the oxide/semiconductor barrier height (Φ_{bs}) (figure 1). They are yield by the following equations :

$$K_1^{o} = 1.5413\ 10^{-6}\frac{m_o}{m_{ox}}\frac{1}{\Phi_{bs}} \quad (2)$$

where, m_o: free electron mass, m_{ox} : effective mass of an electron in the oxide layer ($m_{ox} = 0.5\ m_o$) [22].
It has been shown in [1] that this model is not valid in the inversion regime ($V_g>0$). We should take account of the corrective terms due to temperature, semiconductor interface degeneracy and the Schottky effects (figure 1) (TDSEs) [1]. So, the current (I_{FN}^{semi}), corresponding to electron injection from the semiconductor, can be represented by the FN classical expression $\left(I_{FN}^{o}\left(E_i,\Phi_{bs}^{TDS}\right)\right)$ which is a function of the field (E_i), the potential barrier (Φ_{bs}^{TDS}) at the oxide/semiconductor interface and a corrective factor ($A_m^{TDS}\left(T,\Phi_{bs}^{TDS},E_i,E_{fs}-E_{co}\right)$) including the TDSEs [1] :

$$I_{FN}^{semi} \approx A_m^{TDS}\left(T,\Phi_{bs}^{TDS},E_i,E_{fs}-E_{co}\right)I_{FN}^{o}\left(E_i,\Phi_{bs}^{TDS}\right) \quad (4)$$

where, $A_m^{TDS}\left(T,\Phi_{bs}^{TDS},E_i,E_{fs}-E_{co}\right)$: corrective factor given by the expression presented in [1].
T: temperature.

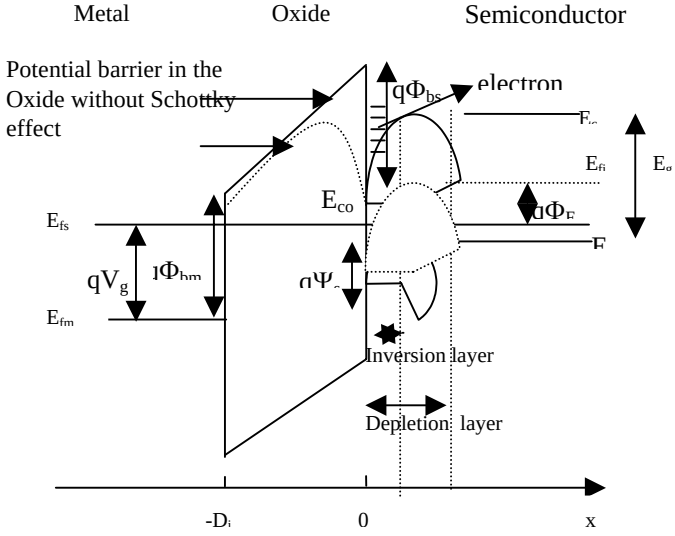

Fig. 1 : Energy band diagram for MOS structure with positively biased metal gate ($V_g>0$) with/without Schottky effect.

In our case, before and after radiation, at ambient temperature and for a potential barrier (Φ_{bs}) value of 3.2 eV [23-26], the parameter ($A_m^{TDS}\left(T, \Phi_{bs}^{TDS}, E_i, E_{fs} - E_{co}\right)$) value is equal to 7.15 and the barrier value $\left(\Phi_{bs}^{TDS}\right)$ is about 3.10 eV.

III-2- Influence of ionising radiation on FN conduction (V_g>0)

III-2-a- Influence of ionising radiation on the I(V_g) characteristics

Figure 2 shows the experimental current-voltage characteristics I(V_g) (V_g > 0) of the MOS structures before and after radiation as a function of oxide thickness. It appears that the I(V_g) characteristics saturate at high voltage and shift towards the positive voltages after radiation. In [5], it has been shown that, in this case, the influence of radiation is negligible on the C(V_g) characteristics. Thus, one can conclude that radiation does not create any charge in the ultra-thin oxide, and that the shift observed on the I(V_g) characteristics is not due to the storage of charges in the oxide layer.

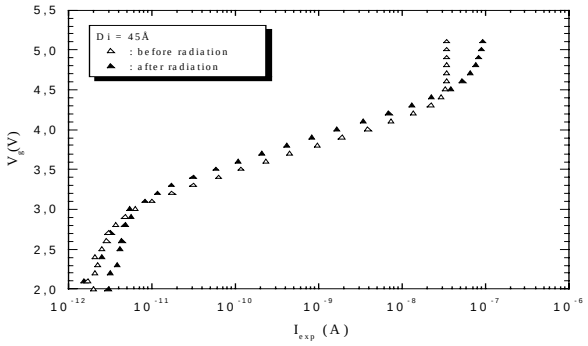

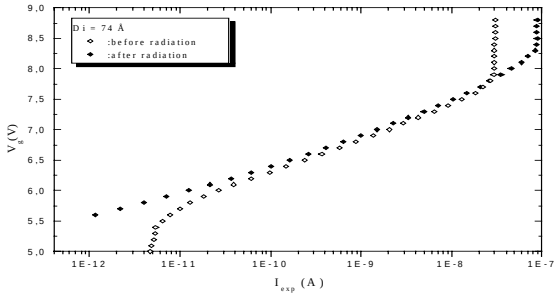

Fig. 2 *:* Typical influence of radiation (7 Mrad dose), according to the oxide thickness, on the current-voltage characteristics of the MOS structure with positively biased gate S = 16 10^{-6}cm².

III-2-b- Modelling of the current-voltage characteristics

Figure 3 shows the FN plots of the experimental current-voltage characteristics, given in Figure 2, without taking account of current saturation at high voltage. On the same figure, the theoretical characteristic that takes account of the TDSEs (relation 4) is also shown. It appears that :

* I(V_g) characteristics are affected by oscillations [27],
* before radiation, the I(V_g) characteristics are affected by the excess current [17,18]. The experimental current is higher than the theoretical one.
* after radiation, the I(V_g) characteristic is practically identical to the theoretical one particularly at high fields for a 74 Å thick oxide layer. For a 45 Å thick layer, the I(V_g) characteristic is close to the theoretical one and affected by the excess current.

The linear behaviour obtained after radiation shows that the conduction is of the FN type. The experimental current can then be represented by the following expression :

$$I_{exp} = S\, K_1^{exp} E_i^2 \exp\left(-\frac{K_2^{exp}\left(\Phi_{bs}^{exp}\right)}{E_i}\right) \qquad (5)$$

where: K_1^{exp} : pre-exponential factor,

$K_2^{exp}\left(\Phi_{bs}^{exp}\right)$: exponential factor depending on the barrier at the oxide/semiconductor interface (Φ_{bs}^{exp}).

Also, the experimental current (I_{exp}) can be modelled using the classical model of the FN conduction and the corrective factor (A_{exp}) due to the TDSEs [1]:

$$I_{exp} = S A_{exp}\left(E_i, \Phi_{bs}^{exp}\right) K_1^{o}\left(\Phi_{bs}^{exp}\right) E_i^2 \exp\left(-\frac{K_2^{exp}\left(E_i, \Phi_{bs}^{exp}\right)}{E_i}\right) \qquad (6)$$

where, $A_{exp}\left(E_i, \Phi_{bs}^{exp}\right)$ is given by :

$$A_{exp} = \frac{K_1^{exp}\left(\Phi_{bs}^{exp}\right)}{K_1^{o}\left(\Phi_{bs}^{exp}\right)} \qquad (7)$$

The conduction parameters (K_1^{exp}, $K_2^{exp}\left(\Phi_{bs}^{exp}\right)$ or the barrier Φ_{bs}^{exp}) obtained are given in Table 1. By taking into account the experimental values of the barrier $\left(\Phi_{bs}^{exp}\right)$, we have listed on the same table, the theoretical values of the factor ($K_1^{o}\left(\Phi_{bs}^{exp}\right)$), the theoretical corrective factor (A_m^{TDS}), and the experimental values of factor (A_{exp}).

Before radiation, the conduction parameter values are lower than the ideal ones. This is caused by the excess current due to defects localized in the oxide layer. The comparison between the various values obtained before and after radiation shows a clear improvement of the

interfacial barrier (Φ_{bs}^{exp}) and the corrective factor (A_{exp}) after radiation.

Also, after radiation, and in the case of oxide layer with a thickness of 74 Å, the barrier (Φ_{bs}^{exp}) is almost ideal, and the factor (A_{exp}) is lower than the theoretical one, although the I(V_g) characteristic obtained is very close to the theoretical one (figure 3). We think that this behaviour can result from a weak shift between the experimental I(V_g) characteristic and the theoretical one. This may be due to the presence of excess current at low field. However, for an oxide with a thickness of 45 Å these parameters are much lower than the ideal ones. This is due to the excess current, which has not been eliminated after radiation.

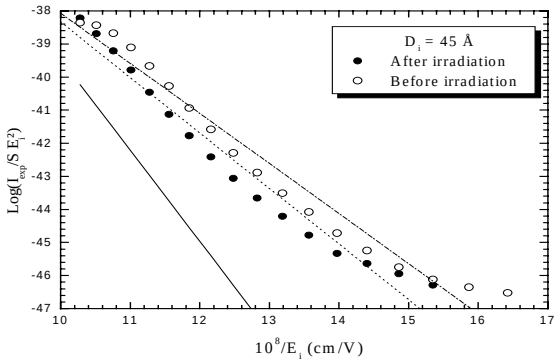

Fig. 3 : Typical FN plots of the experimental current-voltage characteristics for 45Å and 74 Å thick oxide layers. S = 16 10^{-6} cm²,
(-.-.-) fitting of the characteristic before radiation,
(.….) fitting of the characteristic after radiation,
(——) theoretical current (expression 4),

III-3- Influence of radiation on the excess current ($V_g > 0$)

III-3-a- Determination of the excess current

The excess current (I_{exc}) is determined by the following expression [17,27]:

$$I_{exc} = I_{exp} - I_{FN}\left(A_m^{TDS}, K_1^o, \Phi_{bs}\right) \qquad (8)$$

where, $I_{FN}\left(A_m^{TDS}, K_1^o, \Phi_{bs}\right)$:

the FN current determined by using the ideal conduction parameters ($\Phi_{bs} \approx 3.2\,eV$ [23-26], $K_1^o = 10^{-6}$ A/V², $A_m^{TDS} = 7.15$). I_{exp}: the experimental current.

Typical plots of the excess current as a function of the electrical field in the oxide are shown in Fig. 4 for an oxide layer with a thickness of 45 Å before and after radiation, and for a 74 Å thick oxide layer before radiation. For the latter oxide, the excess current is lower than 10^{-11}A after radiation. One can conclude that the excess current increases with decreasing oxide thickness before radiation. This behaviour has been interpreted in [1,17,18] by the increase of the defect area when the oxide thickness decreases. For a 45 Å thick layer, we can conclude that radiation decreases the excess current.

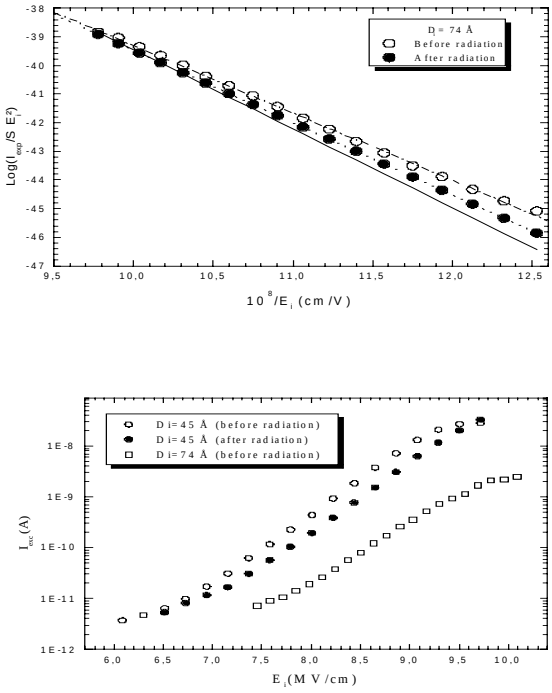

Fig. 4 : Typical influence of radiation on the excess current as function of the oxide field. S = 16 10^{-6} cm².

III-3-b- Excess current modelling

We analysed the effect of radiation on the excess current for MOS structures where the oxide thickness is equal to 45 Å and the excess current significant.

Figure 5 shows the FN plot of each characteristic given in Fig. 4 for a 45 Å thick layer. It can be seen that the linear behaviour is affected by oscillations. Thus, the excess current is of the FN type before and after radiation. The excess current (I_{exc}) can therefore be expressed, according to the oxide field (E_i) and the conduction parameters of defects (K_1^{def}) and $K_2^{def}\left(\Phi_{bs}^{def}\right)$ which is a function of the effective defects barrier $\left(\Phi_{bs}^{def}\right)$ as follows :

$$I_{exc} = S\,K_1^{def}\,E_i^2\,\exp\left(-\frac{K_2^{def}\left(\Phi_{bs}^{def}\right)}{E_i}\right) \qquad (9)$$

where, K_1^{def} : pre-exponential factor of FN conduction, $K_2^{def}\left(\Phi_{bs}^{def}\right)$: exponential factor of FN conduction, given by :

$$K_2^{def} = 6.828\ 10^7 \sqrt{\frac{m_{ox}}{m_o}} \left(\Phi_{bs}^{def}\right)^{3/2} \qquad (10)$$

We derived the conduction parameters (K_1^{def}, $K_2^{def}\left(\Phi_{bs}^{def}\right)$ or the barrier Φ_{bs}^{def}) from Fig 5. The values obtained are listed in table 2. By taking account of the value of the defect barrier (Φ_{bs}^{def}), we have calculated and listed in table 2, the theoretical values of factor ($K_1^{od}\left(\Phi_{bs}^{def}\right)$) following Eq. 2, and the corrective factor ($A_m^{dTDS}\left(\Phi_{bs}^{def}, E_{fs} - E_{co}\right)$) [1] due to the TDSEs.

By taking into account the general expression (Eq. 4) of the FN conduction including the TDSEs, the excess current (I_{exc}) can be modelled by the following expression [1] :

$$I_{exc} = S^d\ A_m^{dTDS}\ K_1^{od}\ E_i^2 \exp\left(-\frac{K_2^{od}\left(\Phi_{bs}^{def}\right)}{E_i}\right) \qquad (11)$$

where, S^d: the effective defect area is given by the procedure described in [1].

Considering the barrier $\left(\Phi_{bs}^{def}\right)$, we have determined and listed in table 2, the effective area of defects (S^d) before and after radiation. The results show that radiation improves the defect characteristics: the barrier increases by 6.5 % and the defects area decreases by 68 %. These major results show that radiation greatly impacts the defects in the oxide layer. Indeed, the reduction of the defect area after radiation shows that radiation is the cause of this reduction of defects in the oxide layer.

In addition, since the radiation does not affect the excess current in the case of electron injection from the metal [5], it can be concluded that radiation can directly or indirectly impact the defects in the ultra-thin oxide adjacent to the oxide /semiconductor interface. As a result, the shift of the $I(V_g)$ characteristics after radiation (Fig. 2) can be interpreted in terms of improvement of the MOS electrical properties after radiation: reduction of defects close to the oxide/semiconductor interface in the oxide and due to technological process. For a 74 Å thick oxide layer, radiation eliminates almost all these defects close to the oxide/semiconductor interface.

In [1] two assumptions have been made regarding the depth of defects: depth is identical to the oxide thickness, or these defects are localized in the middle of the oxide layer. Since, we have found in this section that the radiation has an influence on the defects close to the oxide/semiconductor interface, we can conclude that the depth is in favour of the first hypothesis: depth is identical to the oxide thickness. Also, these interesting results enable us to confirm the results obtained previously by analysing the oscillations of the excess current [27].

It should be noted that the radiation influence on the defects is interpreted in terms of dependence of the excess current on the oxide thickness (when the oxide thickness decreases, the excess current increases [17]). This is more noticeable on the 74 Å thick oxide layer because there are less defects than in the case of thin 45 Å thick oxide layer.

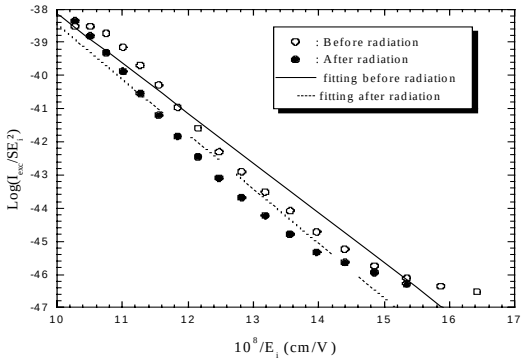

Fig. 5 : Fowler-Nordheim Plots of the excess current before and after radiation. S=16 10^{-6}cm², D_i = 45 Å.

III-4- Influence of radiation on the breakdown field

The current-voltage characteristics obtained in the inversion regime (Fig 2) present a saturation at high voltage. So, we cannot bias the structures to breakdown. To analyse the radiation influence on the breakdown field, we have biased the structures in the accumulation regime (V_g<0) and determined the field breakdown. Figure 6 shows, based on oxide thickness, the Gumbel distributions of the breakdown field before and after radiation. One can derive that radiation degrades the extrinsic breakdown field (low field), particularly for a 74 Å thick oxide layer. However, the intrinsic breakdown field (high field) undergoes a slight degradation. In this case, the breakdown field (E_{BD}) taken as a 75% failure rate degrades by 4% (1.6%) when the oxide thickness is equal to 74 Å (45 Å).

With respect to the electrons injection from the metal (V_g<0) [17], we have found that the breakdown field is directly or indirectly related to the defects in the oxide layer: when the effective area of these defects increases the breakdown field decreases. In our case, these results are not applicable after radiation, because we found that the defect area decreases and the breakdown field value degrades after radiation**.** These results are in good agreement with those obtained in [4].

Therefore, it can be concluded that the mechanism causing for breakdown degradation after radiation could be

due to other causes but not to defects localized in the oxide layer. These results are in good agreement with those published in [4]: radiation induces traps, which create the percolation path in the gate oxide at breakdown or soft breakdown. From our results, this path becomes more important as the oxide thickness increases and cannot affect the FN conduction mechanism.

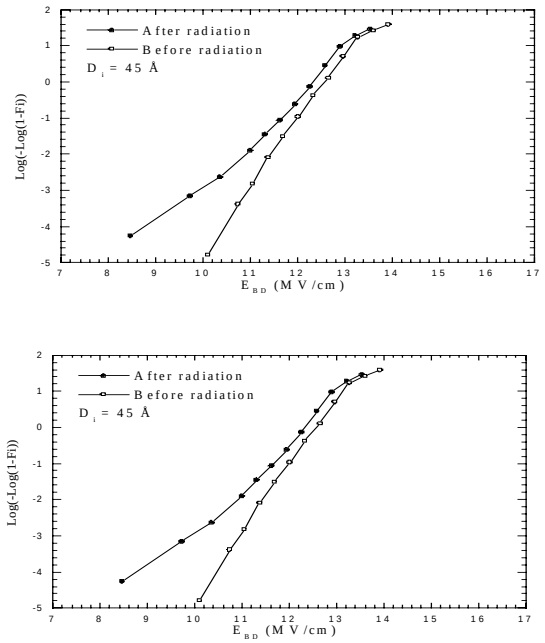

Fig. 6 : Gumbel distributions of breakdown field before and after radiation (7 Mrad (Si) dose). S = 16 10^{-6} cm².

IV- CONCLUSION

From the analysis of the influence of radiation on the experimental current-voltage characteristics ($V_g > 0$) of MOS structures in the oxide layer less than 100 Å thick, it can be concluded that radiation fails to create a charge in the oxide layer, but improves conduction parameters and reduces the excess current due to defects in the oxide layer. This current is practically eliminated after radiation in 74 Å thick oxides and greatly reduced in 45 Å thick oxides where the improvement of conduction parameters has been attributed to the improved defect characteristics: the barrier increases by 6.5 % while the area decreases by 68 %. Comparing these results with those previously obtained [27], it appears that the defect depth is almost the same as the oxide thickness, and that radiation reduces defects close to the oxide/semiconductor interface.
By reviewing the radiation influence on the breakdown distributions, we were able to derive that radiation degrades the breakdown field distributions. This shows that, after radiation, the presence of defects in the oxide and the degradation of the breakdown field are not related.

However, this degradation can be interpreted by the formation of the percolation path in the oxide layer after radiation. This path cannot affect the FN conduction mechanism.

[1] Y. Khlifi, K. Kassmi, R. Maimouni, Eur Phys. Eur. Phys. J. appl. Phys. **28**, 27-41, 2004
[2] A. Concannon, S. Keeney, A. Mathewson, R. Bez, C. Lombardi, IEEE Transactions on Electron Devices. Vol.40, N7, p.1258, July 1993
[3] H. Fukuda, T. Hayashi, A. Uchiyama, T. Iwabuchi, Electronics letters, Vol.**29**, N11, p.947, 1993.
[4] M. Houssa, S De Gendt, P de Bokx, P W Mertens and M M Heyns, Semicond. Sci. Technol. **14**, P.741-746, 1999.
[5] K. Kassmi, R. Maimouni, G. Sarrabayrouse, Eur. Phys. J. AP **8**, p. 171-178, 1999.
[6] E. Iliescu, C. Codreanu, M. Badila, V. Banu, A. Badoiu, NIM B (**161-163**), p. 381-386, 2000.
[7] E. A de Vasconcelos and E. F da Silva Jr, Semicond. Sci. Technol. **12**, p.1032-1037, 1999.
[8] A. Candelori, A. Paccagnella, A. Scarpa, G. Ghidini, P. G. Fuochi, Microelectronics Reliability, **39**, p. 227-233, 1999.
[9] N. Stojadinovic, S. Golubovic, V. Davidovic, S. Djoric-Velikovic and S. Dimitrijev, Physica. Status. Solidi (a), **169**, 63 (1998).
[10] S. Kaschieva, I. Yourukov, NIM B (**170**), p. 385-388, 2000.
[11] S. Kaschieva, I. Yourukov, Solid-State Electronics, **42**, p.1835-1838, 1998.
[12] N.S. Saks, M.G. Ancona, J.A. Modolo, IEEE Trans. Nucl. Sci. **NS-33**, 1185,1986.
[13] M. Walters, Reisman, J.Appl. Phys. **67**, 2992,1990.
[14] B. J. Cho, S. J. Kim, C. H. Ling, Moon-Sig Joo, In-Seok Yeo, Solid-State Electronics, **44**, p.1289-1292, 2000.
[15] C H Ang, C H Ling, Z Y Cheng, S J Kim and B J Cho, Semicond. Sci. Technol. **15**, p. 961-964, 2000.
[16] M. Lenzlinger and E. H. Snow, J. Appl. Phys, **40**, 278 (1969).
[17] Y. Khlifi, K. Kassmi, L. Roubi, R. Maimouni, Eur Phys. Journal of Applied Physics **9**, March p. 239-246, 2000 .
[18] Y. Khlifi, PH D Thesis, 'Université Mohamed Premier', Oujda, Morocco, N°33, 2001.
[19] A. Aziz, K. Kassmi, F. Olivié, Nanotechnology **15**, p. 237 – 242, 2004 .
[20] A. Aziz, K. Kassmi, Ka. Kassmi, F. Olivié, Semicond. Sci. Technol. **19**, p. 877–884 , 2004.
[21] G. Sarrabayrouse, F. Compabadal, J. L. Prom, IEE Proc, 36, Pt. G, P.215, 1989.
[22] Z.A. Weinberg, J. Appl. Phys, **53**, p. 5052, 1982.
[23] Christopher J. Hegarty, Jack C. Lee and Chenming Hu, Solid-state Electronics, **34** (11), p. 1207-1213, 1991.
[24] Seiji Horiguchi, Hideo Yoshino, J. Appl. Phys. **58** (4), 1985.
[25] Sheng S. Gong, Marie E. Burnham, N. David Theodore, Dieter K. Schroder, Fellow, IEEE Transactions on Electron Devices, ED-**40** (7) 1993.
[26] Z. A. Weinberg, M. V. Fischetti, J. Appl. Phys. **57** (2), 1985.
[27] Y. Khlifi, K. Kassmi, L. Roubi, R. Maimouni, Physica Status Solidi A **182**, 737, 2000.

	D_i (Å)	*Experimental conduction parameters*		*Theoretical parameters*		
		$\cdot_{bs}^{exp}$ (eV)	K_1^{exp} (A/V²)	K_1^{o} (A/V²)	A_m^{TDS}	A_{exp}
Before radiation	45 74	2.14 2.86	$1.1\ 10^{-10}$ $1.33\ 10^{-7}$	$1.44\ 10^{-6}$ $1.13\ 10^{-6}$	5.03 6.14	$7.34\ 10^{-5}$ 0.016
After radiation	45 74	2.28 3.015	$4.37\ 10^{-10}$ $6.34\ 10^{-7}$	$1.35\ 10^{-6}$ $1.021\ 10^{-6}$	5.293 6.5	$3.23\ 10^{-4}$ 0.62

Table 1 *: Conduction parameters ($\cdot_{bs}^{exp}$, K_1^{exp}) extracted from the I(V_g) characteristics [obtained before and after radiation (Fig. 3)], prefactor (K_1^{o}) calculated from Eq. (2) and barrier values ($\cdot_{bs}^{exp}$), theoretical factor (A_m^{TDS}) due to the TDSEs, and experimental corrective factor (A_{exp}) (Eq. 7).*

	D_i (Å)	*Experimental conduction parameters*		*Theoretical parameters*		S^d (cm²)
		$\cdot_{bs}^{déf}$ (eV)	$K_1^{déf}$ (A/V²)	K_1^{od} (A/V²)	A_m^{dTDS}	
Befor radiati	45	2.13	$8.74\ 10^{-11}$	$1.44\ 10^{-6}$	5.013	$1.93\ 10^{-10}$
Aft radiati	45	2.267	$2.93\ 10^{-10}$	$1.358\ 10^{-6}$	5.27	$6.15\ 10^{-11}$

Table 2 : Conduction parameters of defects ($\cdot_{bs}^{def}$, K_1^{def}) extracted from excess current-voltage characteristics of Fig. 5, prefactor (K_1^{od}) calculated from Eq. (2) and the barrier ($\cdot_{bs}^{def}$) values, corrective factor (A_m^{dTDS}) due to TDSEs, and effective area of defects (S^d).

